Oxidative degradation of clindamycin in aqueous solution using nanoscale zero-valent iron/H_2O_2/US

Mitra Gholami[a], Kourosh Rahmani[b], Ayat Rahmani[c], Hassan Rahmani[d,*], Ali Esrafili[a]

[a]Department of Environmental Health Engineering, School of Health, Iran University of Medical Sciences, Tehran, Iran,
Tel. +98 9123906308; email: gholamimitra32@gmail.com (M. Gholami), Tel. +98 88607945; email: a_esrafily@yahoo.com (A. Esrafili)
[b]Department of Environmental Health Engineering, School of Public Health, Ardabil University of Medical Sciences, Ardabil, Iran,
Tel. +98 33510052; email: krahmanii@yahoo.com
[c]Department of Environmental Health Engineering, School of Health, Shahid Beheshti University of Medical Sciences, Tehran, Iran,
Tel. +98 22432040; email: ayat_rahmani@yahoo.com
[d]Department of Environmental Health Engineering, School of Public Health, Ahvaz Jundishapur University of Medical Sciences,
Ahvaz, Iran, Tel. +98 33738269; Fax: +98 33738282; email: hs.rahmani@yahoo.com

ABSTRACT

In this study, we investigated clindamycin (CLM) removal efficiency by using nanoscale zero-valent iron (nZVI) particles in the presence of hydrogen peroxide and sonolysis process. Laboratory experiments were performed at $21 \pm 2°C$. Also, the effects of initial CLM concentration (45, 80, and 100 mg/L), the molar ratio of H_2O_2 (0.1, 0.5, and 1 mM), nZVI (0.06, 0.1, and 0.2 g/L), pH (3, 7, and 10), in the presence of ultrasonic waves (35 and 130 kHz with 500 W power) were studied. The results demonstrated that the sonolysis process combined with nZVI and H_2O_2 in nZVI/H_2O_2/US system improved the degradation efficiency. Results indicate that the CLM degradation rate increased with decreasing pH and increasing contact time, temperature, nZVI concentration (0.2 g/L), H_2O_2 concentration (to 180 mM), and ultrasound frequency (130 kHz/500 W). The optimal concentration of the H_2O_2, according to the extent of the ·OH scavenging reaction with these reagents, was demonstrated for CLM removal.

Keywords: Clindamycin; Zero valent iron nanoparticles; Hydrogen peroxide; Sonolysis process

1. Introduction

In the last decade, occurrence of pharmaceuticals, typically at levels in the nanograms to low micrograms per liter range, have been reported in the water cycle, including surface waters, wastewater, groundwater, and with a lesser range in drinking water [1]. Advances in analytical technology have been a key factor driving their increased detection. The presence of low concentrations of antibiotics in the environment may result to developing antibiotic resistant bacteria [2]. The majority of these contaminants have low biodegradability [3] and high toxicity [4], showing mutagenic and carcinogenic characteristics [5]. Clindamycin, a broad-spectrum antibiotic, is highly effective against gram-positive and gram-negative anaerobic pathogens and is effectively used

*Corresponding author.

for the treatment of some diseases such as serious respiratory tract, skin and soft tissue infections [6]. Different methods are used for wastewater treatment containing pharmaceutical compounds [7–9]. Among these methods, the advanced oxidation process (AOP) seems to be more practical than other methods such as activated carbon adsorption, reverse osmosis, and air stripping. Biological treatment is applied for wastewater-containing biodegradable substances and non-toxic materials [10,11]. AOPs such as ozonation, UV/H_2O_2, UV/O_3, Fe^{2+}/H_2O_2, and $UV/O_3/H_2O_2$ are widely applied for the degradation of organic compounds in industrial wastewater and groundwater [12]. Several studies have shown that this technology has good ability to oxidize organic pollutants to carbon dioxide and water [13]. Ultrasonic irradiation causes rapid degradation of chemical contaminants in water that has attracted much attention. Sonication of aqueous solutions, motivates the formation and collapse of cavitation bubbles and also subsequent increasing temperature and pressure that contributed to produce the chemical species such as $H\cdot$, $OH\cdot$, $O\cdot$, and H_2O_2. This phenomenon with high energy has led to the destruction of organic compounds in aqueous solutions. Degradation processes may be carried out by two main mechanisms: direct pyrolysis in and around the collapsing bubbles, and oxidation by OH radicals [14]. The ultrasonic process alone is not cost effective due to the high energy consumption and therefore can be used as a pre-oxidant step before the biological treatment. Organic compounds with large atoms are broken by ultrasound, and then go into the biological treatment unit. Ultrasound is also applied in compounding with other technologies to increase the efficiency of degradation. It should be noted that a combination of methods, including sonochemical, sonophotochemical and sonoelectrochemical, may have a better pollutant removal efficiency [15].

In recent years, zero-valant iron nanoparticles have been considered due to its high efficiency in the removal of various contaminants such as heavy metals [16], chlorinated organic [17], nitroaromatic compounds [18], polybrominated diphenyl ethers [19], nitrates [20], pesticides [21], and dyes [22]. Nanoscale zero-valent iron (nZVI) particles gets good reliability to use in environmental remediation, due to its small particle size, large specific surface area, high density, and great intrinsic reactivity of reactive surface sites [23].

A limited number of investigations have been conducted to remove the antibiotic clindamycin from the aquatic environment. Zhu et al. carried out clindamycin's separation and recovery from clindamycin fermentation wastewater with nanofiltration (NF) membranes [24].

No work on removal of clindamycin antibiotic in aqueous solution by $nZVI/H_2O_2/US$ process has been reported. Thus, it is important to assess the efficiency of this process in degradation of clindamycin antibiotic in aqueous solutions. This paper addresses the role of optimal conditions in the $nZVI/H_2O_2/US$ process for clindamycin antibiotic removal from aqueous.

2. Materials and methods

2.1. Reagents

Clindamycin powder and methanol (HPLC grade ≥99.9%) were purchased from Sigma-Aldrich (St. Louis, MO, USA) and acetone (HPLC grade ≥99.98% pure) from Acros Organics Co, (Belgium). Sulfuric acid, sodium hydroxide, potassium iodide, sodium thiosulfate, and starch were prepared from CMC (Germany). H_2O_2 (30% w/w) was obtained from BDH Company and the Whatman filters were from Prolabo, France.

2.2. Preparation of nanosized zero-valent iron particles

The nZVI used in this study was made according to the method described by Zhu et al. [24]. Synthesis with sodium borohydride is a simple laboratory method with simple chemical reagents for the synthesis of nanoscale iron particles that was used in this study. Also, to make ferric chloride solution 0.1 M from powder, use of deionized water neutralized with nitrogen is specified. Furthermore, to make 0.16-M sodium borohydride solution use of 0.1-M sodium hydroxide is definite. After the preparation of solutions, in intense mixing conditions with a tunable mechanical stirrer at 400 rpm, sodium borohydride solution titration was performed with a flow rate of 0.625 mL/s. According to the following reaction, the borohydride was introduced to reduce ferric ion (Fe^{3+}) to zero-valent iron [Fe^0].

$$4Fe^{3+} + 3BH_4^- + 9H_2O \rightarrow 4Fe^0$$
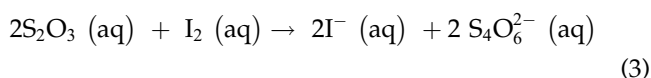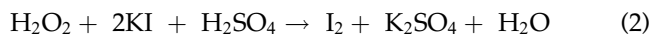$$\downarrow + 3H_2BO_3^- + 12H^+ + 6H_2 \quad (1)$$
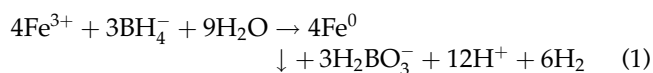
After 30 min of contact time (at $23 \pm 0.5°C$), the obtained iron particles were harvested with vacuum filtration and at the end stabilized with a large volume of deionized water to wash. In order to storage and prevent oxidation of the nanoparticles, a thin layer of ethanol on the top of iron particles can be used. A systematic characterization of nZVI has been performed using transmission electron microscopy (TEM) and X-ray diffraction methods (Philips XRD 3100

diffractometer) (Fig. 1). The characteristic broad peak at 2θ of 45 and 65° indicates that the zero valent iron is predominantly present in the sample. The field emission scanning electron microscope (FESEM) image (Hitachi S4160, Japan) had an excellent high-resolution quality that is particularly valuable when studying particles in the 1–200 μm size range. Images of nano-sized zero-valent iron particles were prepared in the Faculty of Tehran University. These structural features images of nZVI and structural changes were used after the reactions were studied (Fig. 2).

2.3. Examination methods

In this study, clindamycin as a selected antibiotic, with concentrations of 45, 80, and 100 mg/L were added to the reactor includes different concentration of zero valent iron nanoparticles (0.06, 0.1, and 0.2 g/L) and hydrogen peroxide (0.1, 0.5, and 1 mM). Initial pH of clindamycin solution was adjusted using hydrochloric acid and sodium hydroxide by use of pH meter (pHS-3B, Shanghai, China). Ultrasound treatments were carried out using an ultrasound generator (Elma CD-4820, Germany) with 35 and 130 kHz frequencies and input power of 500 W. Then, 5 mL of sample was pulled from the reactor outlet for the analysis over 150 min (in four 30-min intervals). Before injecting the sample into the HPLC, samples were drawn through filters with pore 0.2 μm. Detection of Clindamycin antibiotic was taken at 338 nm by HPLC. Residual hydrogen peroxide in the samples was quantified by the potassium iodide method (Eqs. (2) and (3)).

$$H_2O_2 + 2KI + H_2SO_4 \rightarrow I_2 + K_2SO_4 + H_2O \qquad (2)$$

$$2S_2O_3 \; (aq) \; + \; I_2 \; (aq) \rightarrow \; 2I^- \; (aq) \; + 2 \, S_4O_6^{2-} \; (aq) \qquad (3)$$

The results indicate that hydrogen peroxide remaining in the sample output was not really impressive. Each run took in three replications, and average of results was reported.

2.4. Clindamycin analysis

The most significant physical and chemical properties of clindamycin antibiotic are shown in Table 1. Different concentrations of the antibiotic were determined by HPLC at 338-nm wavelength. The mobile solution consisted of a mixture of 40 and 60% acetonitrile in 10-mM phosphate buffer with pH of 7.5 with a flow rate of 1.0 mL/min and 20-μL injection.

3. Results and discussion

3.1. Effect of zero iron nanoparticles concentration

At first, the effect of zero iron nanoparticle concentration on clindamycin removal was investigated. After being separated, the nanoparticles were suspended in an aqueous solution of ethanol (nZVI concentration was 100 g/100 mL). To add specific doses of nanoparticles, certain volume of suspension was added to the sample. To prevent the precipitation of nanoparticles in suspension, vessels containing suspension were shacked continuously. Results indicated that with increasing zero iron nanoparticles dosage, removal efficiency increased (43%, in 0.2 g/L zero iron nanoparticles concentration) (Fig. 3). Increasing the
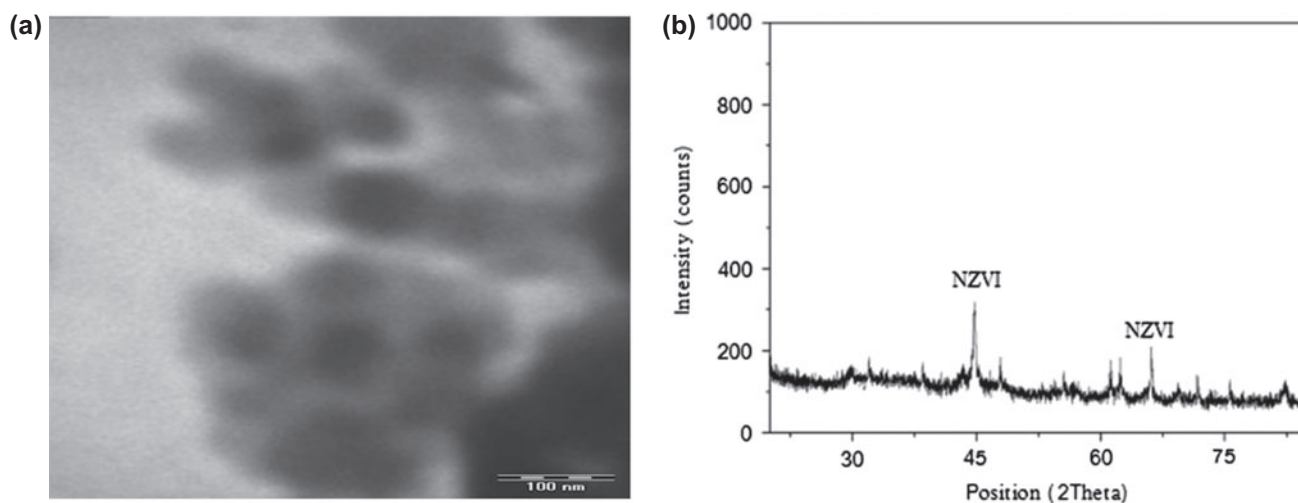

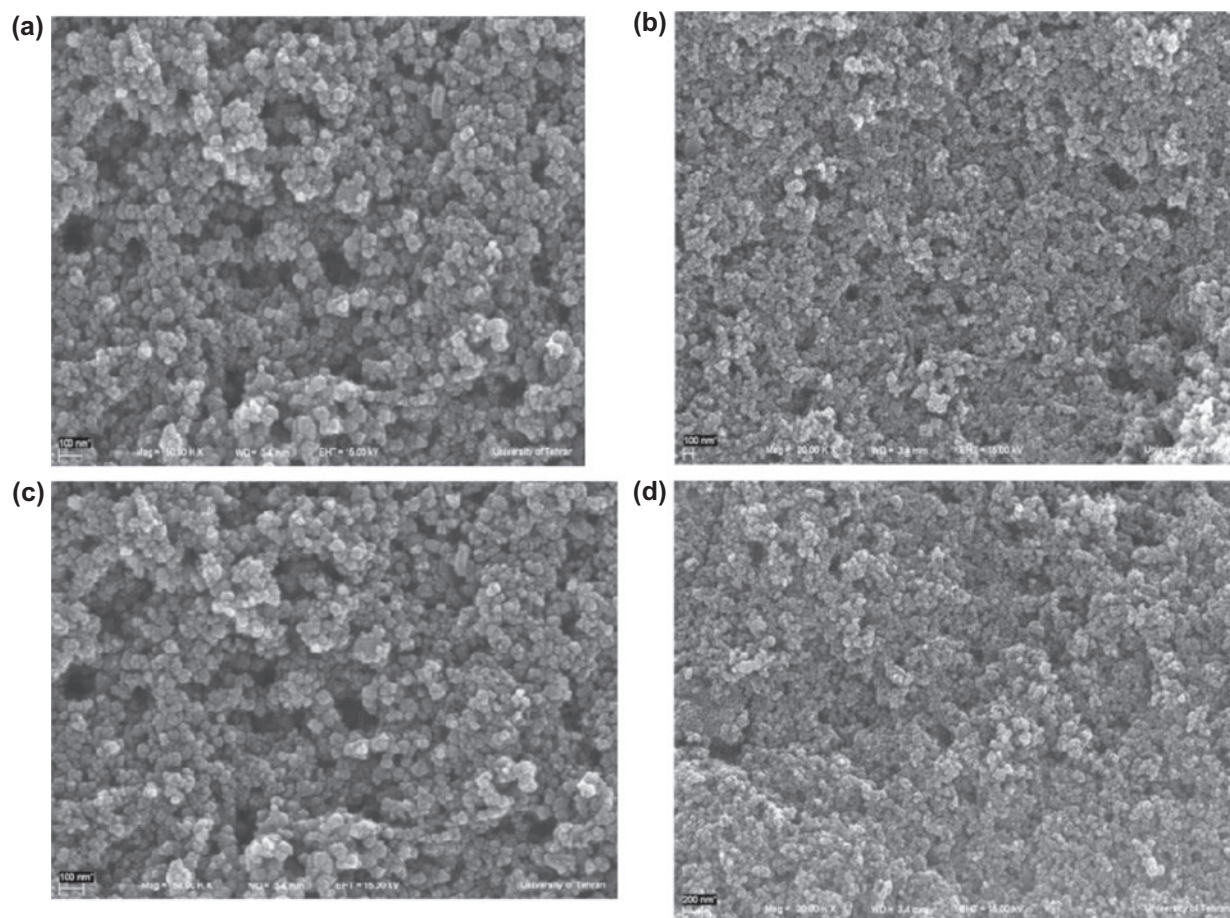Fig. 1. Characterization of NZVI particles: (a) TEM and (b) XRD.

Fig. 2. FESEM image from Fe^0 particles before (a and c) and after (b and d) the reaction.

Table 1
Clindamycin antibiotic physical and chemical structure

Molecular formula	$C_{18}H_{33}ClN_2O_5S$
Molecular weight (g mol^{-1})	424.9830
Melting point (°C)	255°C
Solubility in water	30.6 g L^{-1}
Molecular structure	

sites for hydrogen peroxide decomposition and production of more reactive oxidants such as hydroxyl radicals, result in increased selected antibiotic removal efficiency. In other words, we can say that with an increasing nZVI dosage, total surface area and therefore adsorption increases on active [25]. It is attributed to the agglomeration of nZVI particles and the scavenging of hydroxyl radicals through undesirable reaction [26].
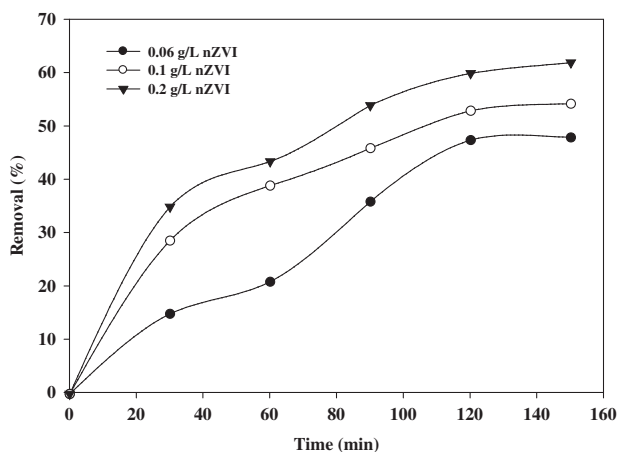
$$Fe^{2+} + \cdot OH \rightarrow Fe^{3+} + OH^- \tag{4}$$

Fig. 3. Effect of zero iron nanoparticle concentration on clindamycin removal efficiency (1 mM H_2O_2, CLM = 45 ppm, pH 7, and US frequency = 130 kHz).

3.2. Effect of hydrogen peroxide concentration

After regulating the optimal absorption of zero valent iron nanoparticles (nZVI = 0.2 g/L, CLM = 45 ppm, pH 7, and US = 130 kHz) the consequence of hydrogen peroxide concentrations (0.1, 0.5, and 1 mM) was examined (Fig. 4). Results demonstrated that with increasing hydrogen peroxide concentration, the removal efficiency similarly increased (73%). This was due to the increase in hydroxyl radical production. However, the excess OH radicals tended to react with other OH radicals and excess hydrogen peroxide. Therefore, the degradation may decrease due to the scavenging effect of hydroxyl radicals and the inhibition of iron corrosion by hydrogen
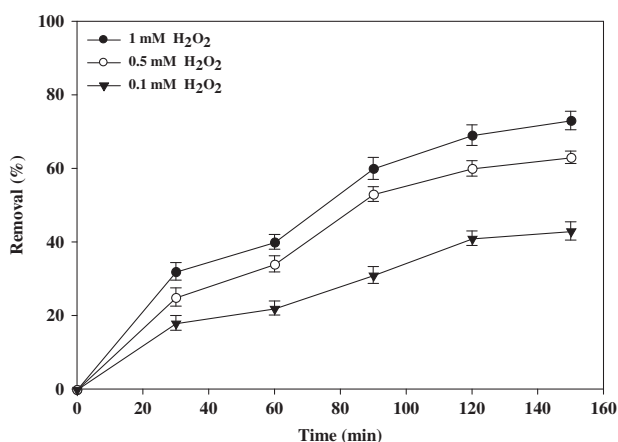

Fig. 4. Effect of hydrogen peroxide concentrations on clindamycin removal efficiency (nZVI = 0.2 g/L, CLM = 45 ppm, pH 7, and US = 130 kHz).

peroxide [27]. The results are in agreement with other studies using Fenton process for the treatment of azo reactive dyes [28,29].

Since the presence of excess hydrogen peroxide in the environment, (which is a less active than hydroxyl radicals) [30] in this study, the optimum concentration of hydrogen peroxide was considered as 1 mM (Table 2).

3.3. Effect of initial pH

This work examined the issue of initial pH on the removal of clindamycin, by the nZVI/H_2O_2/US process. The initial pH was set at 3, 7, and 9. The results are shown in Fig. 5. In initial antibiotic concentration, decreasing pH had a positive impact on nZVI/H_2O_2/US process in the removal of clindamycin. pH is an important element that involves the performance of Fenton and Fenton-like operations. Moreover, the corrosion of zero valent iron was greatly influence by H^+ concentration [31,32]. More subject areas have shown that acidic pH between 3 and 4 is the best range of pH for the Fenton reaction. This result is in accordance with other works of literature [33,34]. Although, some researchers think the higher pH may also have significant reactivity. But at higher pH and alkaline environments, will cause the reaction of H_2O_2 decomposition more limited [35]. This is imputable to its controlling role in the catalytic activity, stability, H_2O_2 activity, and iron spikes. Likewise, the oxidation ability of hydroxyl radicals in acidic conditions is stronger [36]. Above the optimum pH value, there may be a possible decomposition of H_2O_2 into water and oxygen and also the possible deactivation of the catalyst for the formation of the other complexes leading to a reduction of OH· radicals [37]. Also, it is experienced that the acid condition favors the dissolution of iron power, and more Fe^{2+} was produced under acidic condition. So, that was celebrated the highest removal efficiency at pH 3 [38].

3.4. Effect of ultrasonic irradiation

The effect of different irradiations (35 and 130 kHz) in power of 500 W was evaluated by ultrasonic bath without adding nanoiron and hydrogen peroxide. The clindamycin removal efficiency was significantly decreased with the decreasing of ultrasonic irradiation (Fig. 6). Increasing the ultrasonic power will increase the energy of cavitation, decreasing the threshold limit of cavitation and enhance the quality of cavitation bubbles [39]. With increasing the ultrasonic irradiation, the reaction rate of hydroxyl radical

Table 2
Electrical energy consumption at ultrasonic bath with 500 W of power

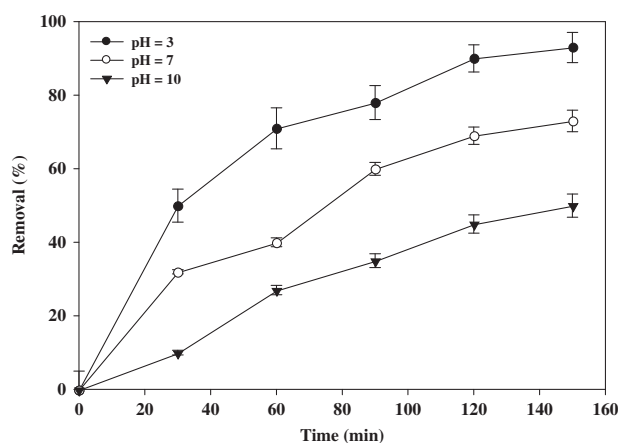| Time (min)	pH 7 H$_2$O$_2$ = 0.5 mM C$_0$ = 45 mg L^{-1} nZVI (g)			pH 7 nZVI = 0.2 g C$_0$ = 45 mg L^{-1} H$_2$O$_2$ (mM)			nZVI = 0.2 g H$_2$O$_2$ = 1 mM C$_0$ = 45 mg L^{-1} pH		nZVI = 0.2 g H$_2$O$_2$ = 1 mM pH 3 C$_0$ (mg L^{-1})	
	0.06	0.1	0.2	0.1	0.5	1	3	10	80	100
30	94.6	47.3	35.3	37.3	31.4	26.6	12.6	54.0	16.5	21.0
60	126.1	74.1	63.0	75.7	42.0	34.4	14.2	5.8	16.8	21.0
90	141.9	89.9	70.9	70.9	35.4	29.1	17.4	70.9	21.8	59.4
120	137.6	89.0	68.8	68.8	38.7	30.2	15.1	8.6	20.4	31.5
150	157.6	99.5	78.8	85.9	43.9	33.7	156.6	75.7	23.0	31.5

Fig. 5. Effect of pH on clindamycin removal efficiency (nZVI = 0.2 g/L, CLM = 45 ppm, 1 mM H$_2$O$_2$, and US = 130 kHz).
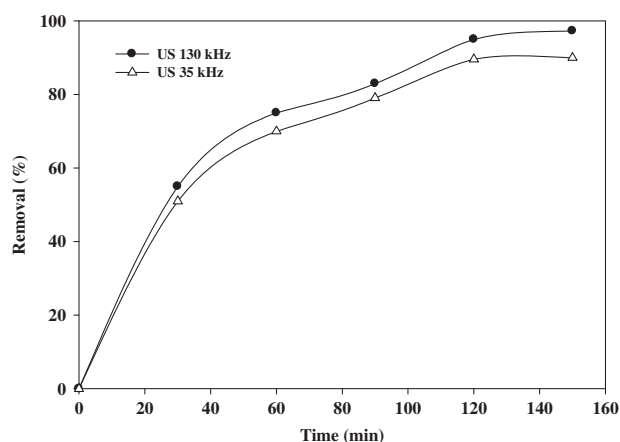

Fig. 6. Frequency effect (nZVI = 0.2 g/L, pH 3, CLM = 45 ppm, and 1 mM H$_2$O$_2$) on clindamycin removal efficiency.

(production of hydrogen peroxide and decomposition of antibiotics) increases. The difference decomposition rate between these two frequencies is due to the low efficiency of production of hydroxyl radicals and possible less departure of these radicals from cavitation bubbles into the solution at a frequency of 35 kHz [40]. In another study, Kim et al. obtained similar results in degradation of dibenzothiophene by ultrasound [41]. Therefore, 130 kHz was selected as an optimum frequency.

3.5. Influence of initial concentration of clindamycin

After determining the optimum dosage, frequency, and pH (nZVI = 0.2 g/L, CLM = 45 ppm, 1 mM H$_2$O$_2$), the effect of clindamycine concentration was studied (the initial Clindamycin concentration was varied from 45, 80 to 100 ppm). The experimental results showed that with increasing clindamycin concentration in the reactor, removal efficiency decreased as shown in Fig. 7. The hydroxyl radical production is not increased in a fixed condition and will remain constant. So with increasing amount of the pollutants, because of hydroxyl radical reduction, the clindamycin removal efficiency will decrease [42,43].

3.6. Clindamycin removal efficiency of non-presence of H$_2$O$_2$, US, and nZVI in the system

In this section, the oxidation efficiency of clindamycin removal was studied in non-presence of H$_2$O$_2$, US, and nZVI in the system. The initial concentrations of CLM, H$_2$O$_2$, nZVI, and pH were fixed at the optimal conditions. Fig. 8 shows the oxidation efficiency of CLM in absence of H$_2$O$_2$, US, or nZVI in the system. From Fig. 8, it can be seen that the CLM oxidation efficiency gets lower with absence of H$_2$O$_2$, US, or nZVI in the system.
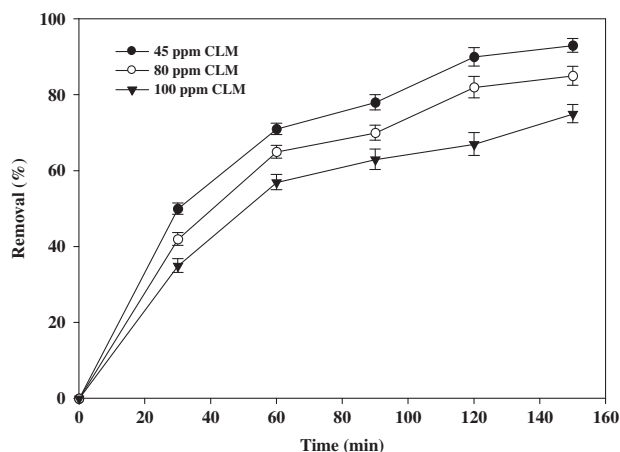
Fig. 7. Effect of clindamycin concentrations (nZVI = 0.2 g/L, 1 mM H_2O_2, and US = 130 kHz) on removal efficiency.

Indeed, there is a synergistic effect between the intended factors (US, nZVI, and H_2O_2). The presence of ultrasonic irradiation not only improved mass transfer significantly, but also activated surface reaction in a heterogeneous system by the generated shock wave which could increase solubility of Fe^{2+} and accelerate the degradation of organic pollutants [44]. Also, because of the high specific area in nZVI, the concentration of active sites could be extremely high as well, that dramatically increases the catalytic activity of the system [45,46]. In the absence of hydrogen peroxide, the system could not generate enough hydroxyl radicals, and thus the degradation rate and efficiency were logically low [47].
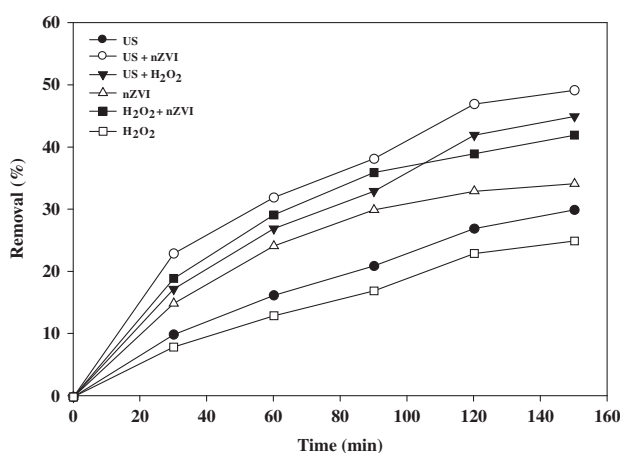
3.7. COD removal efficiency

The effect of time at three different H_2O_2 concentrations (and other fixed parameters optimized conditions, i.e. nZVI = 0.2 g/L, pH 3, and CLM = 45 ppm) on chemical oxygen demand (COD) removal is shown in Fig. 9. Analysis indicated COD reduction in optimal conditions of the combined systems applied in this study. COD was determined according to the Standard Methods [42]. To avoid interruptions of H_2O_2, in the COD determination, the pH was adjusted to above 10 to decompose H_2O_2 to oxygen and water [48]. Similar results have been obtained in other studies [49].

3.8. Ultrasonic bath electrical energy consumption

The amount of electrical energy consumed by the ultrasonic bath for selected antibiotic removal is calculated from the following equation [48]:

$$\left[\text{EE/O} = \frac{P \times (t/3,600) \times 3,785}{V \times \log(C_0/C)} \right]$$

In which, P is the ultrasonic power (kW), t is the reaction time (s), V is the reactor volume (L), C_0 and C are the clindamycin initial and effluent concentration. According to the obtained results, in optimal conditions, the electrical energy consumption is much less than other test conditions (Table 1). Increasing hydrogen peroxide concentration reduces the electrical energy consumption. The significant reduction is observed in the pH 3.
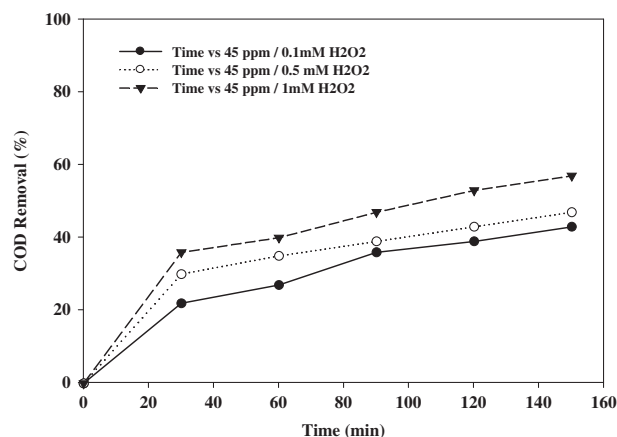

Fig. 8. Clindamycin removal efficiency of non-presence of H_2O_2, US, and nano-ZVI in the system.

Fig. 9. The effect of time at three different H_2O_2 concentrations on COD removal efficiency (nZVI = 0.2 g/L, pH 3, CLM = 45 ppm).

4. Conclusions

This study investigated the clindamycin antibiotic removal efficiency of the hybrid process of nZVI/H$_2$O$_2$/US under different conditions. Results indicated that the system had the most efficiency at lower clindamycin concentrations, acidic conditions, 0.2 g/L concentrations of zero iron nanoparticles and 1 mM H$_2$O$_2$ and maximum contact time. Hydroxyl radicals had a major role in the removal of the antibiotic clindamycin. The presence of both zero iron nanoparticles and hydrogen peroxide was critical to the formation of ion exchange and energetic hydroxyl radicals. From these findings, it can be concluded that nZVI/H$_2$O$_2$/US combined process is effective for removing clindamycin and similar antibiotic.

References

[1] K.-J. Choi, S.-G. Kim, C.-W. Kim, S.-H. Kim, Determination of antibiotic compounds in water by on-line SPE-LC/MSD, Chemosphere 66 (2007) 977–984.

[2] M.V. Walter, J.W. Vennes, Occurrence of multiple-antibiotic-resistant enteric bacteria in domestic sewage and oxidation lagoons, Appl. Environ. Microbiol. 50 (1985) 930–933.

[3] M.L. Richardson, J.M. Bowron, The fate of pharmaceutical chemicals in the aquatic environment, J. Pharm. Pharmacol. 37 (1985) 1–12.

[4] K. Kümmerer, A. Al-Ahmad, V. Mersch-Sundermann, Biodegradability of some antibiotics, elimination of the genotoxicity and affection of wastewater bacteria in a simple test, Chemosphere 40 (2000) 701–710.

[5] A. Bendesky, D. Menéndez, P. Ostrosky-Wegman, Is metronidazole carcinogenic? Mutat. Res. 511 (2002) 133–144.

[6] C.-M. Liu, Y.-K. Chen, T.-H. Yang, S.-Y. Hsieh, M.-H. Hung, E.T. Lin, High-performance liquid chromatographic determination of clindamycin in human plasma or serum: Application to the bioequivalency study of clindamycin phosphate injections, J. Chromatogr., B: Anal. Technol. Biomed. Life Sci. 696 (1997) 298–302.

[7] K. Rahmani, M.A. Faramarzi, A.H. Mahvi, M. Gholami, A. Esrafili, H. Forootanfar, M. Farzadkia, Elimination and detoxification of sulfathiazole and sulfamethoxazole assisted by laccase immobilized on porous silica beads, Int. Biodeterior. Biodegrad. 97 (2015) 107–114.

[8] H. Rahmani, M. Gholami, A. Mahvi, M. Alimohammadi, G. Azarian, A. Esrafili, K. Rahmani, M. Farzadkia, Tinidazole removal from aqueous solution by sonolysis in the presence of hydrogen peroxide, Bull. Environ. Contam. Toxicol. 92 (2014) 341–346.

[9] M. Farzadkia, K. Rahmani, M. Gholami, A. Esrafili, A. Rahmani, H. Rahmani, Investigation of photocatalytic degradation of clindamycin antibiotic by using nano-ZnO catalysts, Korean J. Chem. Eng. 31 (2014) 2014–2019.

[10] E.S. Elmolla, M. Chaudhuri, Comparison of different advanced oxidation processes for treatment of antibiotic aqueous solution, Desalination 256 (2010) 43–47.

[11] A. Eslami, S. Nasseri, B. Yadollahi, A. Mesdaghinia, F. Vaezi, R. Nabizadeh, S. Nazmara, Photocatalytic degradation of methyl tert-butyl ether (MTBE) in contaminated water by ZnO nanoparticles, J. Chem. Technol. Biotechnol. 83 (2008) 1447–1453.

[12] M.-C. Chang, H.-Y. Shu, H.-H. Yu, An integrated technique using zero-valent iron and UV/H$_2$O$_2$ sequential process for complete decolorization and mineralization of C.I. Acid Black 24 wastewater, J. Hazard. Mater. 138 (2006) 574–581.

[13] R. Venkatadri, R.W. Peters, Chemical oxidation technologies: Ultraviolet light/hydrogen peroxide, Fenton's reagent, and titanium dioxide-assisted photocatalysis, Hazard. Waste Hazard. Mater. 10 (1993) 107–149.

[14] D. Drijvers, H. Van Langenhove, M. Beckers, Decomposition of phenol and trichloroethylene by the ultrasound/H$_2$O$_2$/CuO process, Water Res. 33 (1999) 1187–1194.

[15] C. Wu, X. Liu, D. Wei, J. Fan, L. Wang, Photosonochemical degradation of phenol in water, Water Res. 35 (2001) 3927–3933.

[16] M. Dickinson, T.B. Scott, The application of zero-valent iron nanoparticles for the remediation of a uranium-contaminated waste effluent, J. Hazard. Mater. 178 (2010) 171–179.

[17] H. Song, E.R. Carraway, Catalytic hydrodechlorination of chlorinated ethenes by nanoscale zero-valent iron, Appl. Catal., B 78 (2008) 53–60.

[18] X. Zhang, Y.-M. Lin, Z.-L. Chen, 2,4,6-Trinitrotoluene reduction kinetics in aqueous solution using nanoscale zero-valent iron, J. Hazard. Mater. 165 (2009) 923–927.

[19] Y.-H. Shih, Y.-T. Tai, Reaction of decabrominated diphenyl ether by zerovalent iron nanoparticles, Chemosphere 78 (2010) 1200–1206.

[20] W. Wang, Z.-H. Jin, T.-L. Li, H. Zhang, S. Gao, Preparation of spherical iron nanoclusters in ethanol–water solution for nitrate removal, Chemosphere 65 (2006) 1396–1404.

[21] D.W. Elliott, H.-L. Lien, W.-X. Zhang, Degradation of lindane by zero-valent iron nanoparticles, J. Environ. Eng. 135 (2009) 317–324.

[22] Y.-T. Lin, C.-H. Weng, F.-Y. Chen, Effective removal of AB24 dye by nano/micro-size zero-valent iron, Sep. Purif. Technol. 64 (2008) 26–30.

[23] Y.-T. Wei, S.-C. Wu, C.-M. Chou, C.-H. Che, S.-M. Tsai, H.-L. Lien, Influence of nanoscale zero-valent iron on geochemical properties of groundwater and vinyl chloride degradation: A field case study, Water Res. 44 (2010) 131–140.

[24] A. Zhu, W. Zhu, Z. Wu, Y. Jing, Recovery of clindamycin from fermentation wastewater with nanofiltration membranes, Water Res. 37 (2003) 3718–3732.

[25] J. Ramirez, F. Maldonado-Hódar, A. Pérez-Cadenas, C. Moreno-Castilla, C. Costa, L. Madeira, Azo-dye orange II degradation by heterogeneous Fenton-like reaction using carbon–Fe catalysts, Appl. Catal., B 75 (2007) 312–323.

[26] L. Xu, J. Wang, A heterogeneous Fenton-like system with nanoparticulate zero-valent iron for removal of 4-chloro-3-methyl phenol, J. Hazard. Mater. 186 (2011) 256–264.

[27] S.K. Singh, W.Z. Tang, Statistical analysis of optimum Fenton oxidation conditions for landfill leachate treatment, Waste Manage. 33 (2013) 81–88.

[28] M. Tokumura, R. Morito, Y. Kawase, Photo-Fenton process for simultaneous colored wastewater treatment and electricity and hydrogen production, Chem. Eng. J. 221 (2013) 81–89.

[29] T. Zhou, Y. Li, J. Ji, F.-S. Wong, X. Lu, Oxidation of 4-chlorophenol in a heterogeneous zero valent iron/H_2O_2 Fenton-like system: Kinetic, pathway and effect factors, Sep. Purif. Technol. 62 (2008) 551–558.

[30] X. Xue, K. Hanna, M. Abdelmoula, N. Deng, Adsorption and oxidation of PCP on the surface of magnetite: Kinetic experiments and spectroscopic investigations, Appl. Catal., B 89 (2009) 432–440.

[31] A. Ghauch, H. Baydoun, P. Dermesropian, Degradation of aqueous carbamazepine in ultrasonic/Fe^0/H_2O_2 systems, Chem. Eng. J. 172 (2011) 18–27.

[32] W. Kuo, Decolorizing dye wastewater with Fenton's reagent, Water Res. 26 (1992) 881–886.

[33] N. Modirshahla, M. Behnajady, F. Ghanbary, Decolorization and mineralization of C.I. Acid Yellow 23 by Fenton and photo-Fenton processes, Dyes Pigm. 73 (2007) 305–310.

[34] D.L. Sedlak, A.W. Andren, Aqueous-phase oxidation of polychlorinated biphenyls by hydroxyl radicals, Environ. Sci. Technol. 25 (1991) 1419–1427.

[35] P.J.D. Ranjit, K. Palanivelu, C.-S. Lee, Degradation of 2,4-dichlorophenol in aqueous solution by sono-Fenton method, Korean J. Chem. Eng. 25 (2008) 112–117.

[36] N. Daud, B. Hameed, Decolorization of Acid Red 1 by Fenton-like process using rice husk ash-based catalyst, J. Hazard. Mater. 176 (2010) 938–944.

[37] X. Wang, L. Wang, J. Li, J. Qiu, C. Cai, H. Zhang, Degradation of Acid Orange 7 by persulfate activated with zero valent iron in the presence of ultrasonic irradiation, Sep. Purif. Technol. 122 (2014) 41–46.

[38] Y. Jiang, C. Pétrier, T. David Waite, Kinetics and mechanisms of ultrasonic degradation of volatile chlorinated aromatics in aqueous solutions, Ultrason. Sonochem. 9 (2002) 317–323.

[39] T.M. Lesko, Chemical Effects of Acoustic Cavitation, Ph.D. Thesis. California Institute of Technology, Pasadena, California, 2004.

[40] T.J. Mason, Sonochemistry and sonoprocessing: The link, the trends and (probably) the future, Ultrason. Sonochem. 10 (2003) 175–179.

[41] I.-K. Kim, C.-P. Huang, P.C. Chiu, Sonochemical decomposition of dibenzothiophene in aqueous solution, Water Res. 35 (2001) 4370–4378.

[42] A.D. Eaton, M.A.H. Franson, Standard Methods for the Examination of Water & Wastewater, twenty-first ed. American Public Health Association, Washington, DC, 2005.

[43] H. Zhang, L. Duan, Y. Zhang, F. Wu, The use of ultrasound to enhance the decolorization of the C.I. Acid Orange 7 by zero-valent iron, Dyes Pigm. 65 (2005) 39–43.

[44] T. Zhou, Y. Li, F.-S. Wong, X. Lu, Enhanced degradation of 2,4-dichlorophenol by ultrasound in a new Fenton like system (Fe/EDTA) at ambient circumstance, Ultrason. Sonochem. 15 (2008) 782–790.

[45] R. Cheng, J.-L. Wang, W.-X. Zhang, Comparison of reductive dechlorination of p-chlorophenol using Fe^0 and nanosized Fe^0, J. Hazard. Mater. 144 (2007) 334–339.

[46] J.T. Nurmi, P.G. Tratnyek, V. Sarathy, D.R. Baer, J.E. Amonette, K. Pecher, C. Wang, J.C. Linehan, D.W. Matson, R.L. Penn, Characterization and properties of metallic iron nanoparticles: Spectroscopy, electrochemistry, and kinetics, Environ. Sci. Technol. 39 (2005) 1221–1230.

[47] H. Zhou, Y. Shen, P. Lv, J. Wang, P. Li, Degradation pathway and kinetics of 1-alkyl-3-methylimidazolium bromides oxidation in an ultrasonic nanoscale zero-valent iron/hydrogen peroxide system, J. Hazard. Mater. 284 (2014) 241–252.

[48] E.S. Elmolla, M. Chaudhuri, M.M. Eltoukhy, The use of artificial neural network (ANN) for modeling of COD removal from antibiotic aqueous solution by the Fenton process, J. Hazard. Mater. 179 (2010) 127–134.

[49] I. Talinli, G. Anderson, Interference of hydrogen peroxide on the standard cod test, Water Res. 26 (1992) 107–110.